Stem Cell Reports
Article

ISSCR

OPEN ACCESS

The epigenetic state of EED-Gli3-Gli1 regulatory axis controls embryonic cortical neurogenesis

Shuang-Feng Zhang,[1,2,3,4,5] Shang-Kun Dai,[2,3,4,5] Hong-Zhen Du,[2,4,5] Hui Wang,[2,3,4,5] Xing-Guo Li,[6] Yi Tang,[7,*] and Chang-Mei Liu[2,3,4,5,*]

[1]School of Life Sciences, University of Science and Technology of China, Hefei 230027, China
[2]State Key Laboratory of Stem Cell and Reproductive Biology, Institute of Zoology, Chinese Academy of Sciences, Beijing 100101, China
[3]University of Chinese Academy of Sciences, Beijing 100049, China
[4]Institute for Stem Cell and Regeneration, Chinese Academy of Sciences, Beijing 100101, China
[5]Beijing Institute for Stem Cell and Regenerative Medicine, Beijing 100101, China
[6]Graduate Institute of Biomedical Sciences, China Medical University, Taichung 40402, Taiwan
[7]Department of Neurology, Innovation Center for Neurological Disorders, Xuanwu Hospital, Capital Medical University, Beijing 100053, China
*Correspondence: tangyi@xwhosp.org (Y.T.), liuchm@ioz.ac.cn (C.-M.L.)
https://doi.org/10.1016/j.stemcr.2022.07.004

SUMMARY

Mutations in the embryonic ectoderm development (EED) cause Weaver syndrome, but whether and how EED affects embryonic brain development remains elusive. Here, we generated a mouse model in which *Eed* was deleted in the forebrain to investigate the role of EED. We found that deletion of *Eed* decreased the number of upper-layer neurons but not deeper-layer neurons starting at E16.5. Transcriptomic and genomic occupancy analyses revealed that the epigenetic states of a group of cortical neurogenesis-related genes were altered in *Eed* knockout forebrains, followed by a decrease of H3K27me3 and an increase of H3K27ac marks within the promoter regions. The switching of H3K27me3 to H3K27ac modification promoted the recruitment of RNA-Pol2, thereby enhancing its expression level. The small molecule activator SAG or *Ptch1* knockout for activating Hedgehog signaling can partially rescue aberrant cortical neurogenesis. Taken together, we proposed a novel EED-Gli3-Gli1 regulatory axis that is critical for embryonic brain development.

INTRODUCTION

The cerebral cortex is a heterogeneous structure where neuronal circuits underlie higher-order brain functions, including cognition, sensory perception, and sophisticated motor control (MuhChyi et al., 2013; Telley et al., 2019). The assembly of a functional neocortex relies on the timely establishment of cell type-specific programs to induce neural stem/progenitor cells (NSPCs) to produce the appropriate number of neurons and glial cells. Neurons are currently thought to be derived from a population of highly specialized neural stem cells known as radial glial cells (RGs). During cortical neurogenesis, RGs undergo symmetric cell division for self-renewal as well as asymmetric cell division to produce a progeny that is either a neuron or an intermediate progenitor cell (IPC). IPCs, residing in the subventricular zone (SVZ), can produce more neurons through neurogenic division. These newborn neurons pass through the intermediate zone to arrive at an appropriate location of the cortical plate to establish the assembly of the sophisticated neural circuitry, which requires precisely timed programs for defining the position and connectivity.

In humans, mutations in the polycomb repressive complex 2 (PRC2), which comprises enhancer of zeste homolog 1/2 (EZH1/2), embryonic ectoderm development (EED), suppressor of zeste 12 protein homolog (SUZ12), can cause developmental disorders and cancers. Pathogenic variants in EED have been linked to Weaver syndrome, a rare disorder characterized by overgrowth, macrocephaly, and intellectual disability (Cohen and Gibson, 2016; Cohen et al., 2015; Smigiel et al., 2018). Mechanistically, PRC2 is a critical chromatin modifier in cell proliferation and differentiation, maintenance of cell identity, and stem cell plasticity (Boyer et al., 2006; Schmitges et al., 2011; Vizan et al., 2015). The catalytic subunit EZH2 and the methyl group-binding factor EED are indispensable components for the PRC2 complex to catalyze histone H3 lysine 27 tri-methylation (H3K27me3) (Montgomery et al., 2005; Shan et al., 2017). However, little is known about the neural mechanism of the PRC2 complex involved in the regulation of cortical neurogenesis. It has been reported that *Ezh2* regulates the balance between self-renewal and differentiation in the cerebral cortex dependent on H3K27me3 (Pereira et al., 2010). However, as the core component of PRC2, EED plays important roles dependent on H3K27me1 or H3K27ac (Ai et al., 2017; Liu et al., 2019a), which hints that EZH2 or EED may have distinct regulation mechanisms. A previous study suggests that PRC2 EED function is distinct from EZH2 function and is required for homeostasis and cortical injury activation in the postnatal and adult SVZ (Sun et al., 2018). In addition, our previous work has shown that the loss of EED impairs postnatal neuronal differentiation and malformation of the dentate gyrus (Liu et al., 2019a). Although these studies suggest an important role of EED in postnatal neurogenesis, the function of EED in early cortical neurogenesis remains largely unknown.

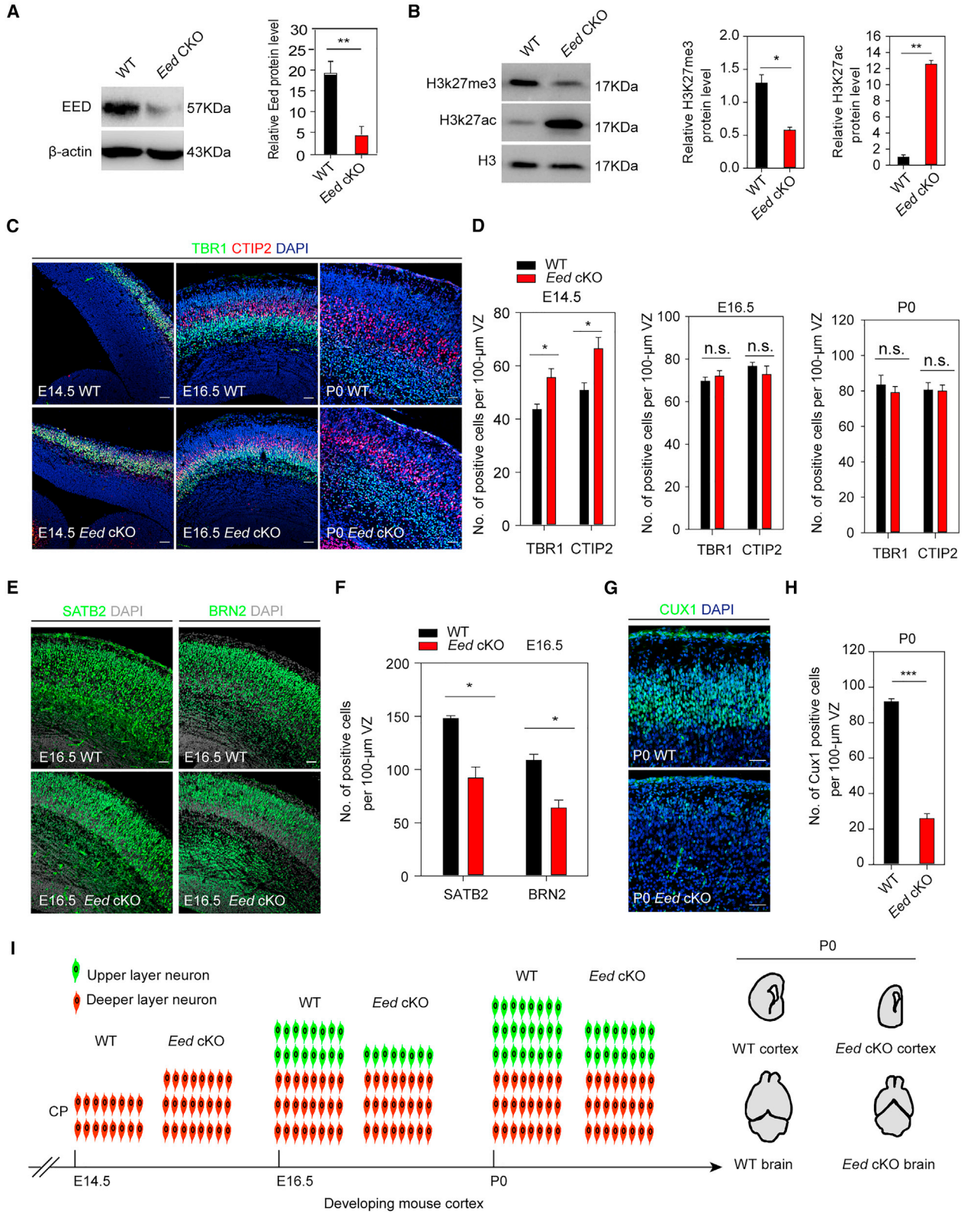

(legend on next page)

Here, by generating stage-specific conditional knockout mice lacking *Eed*, we show that EED regulates the specific gene expression programs to establish neocortical assembly. The essential function of EED in cortical neurogenesis is executed in two manners to orchestrate NSPCs proliferation and differentiation. On the one hand, EED limits neurogenesis and the production of appropriate neurons by repressing differentiation-promoting genes. On the other hand, EED maintains the proliferation and self-renewal of NSPCs through the EED-*Gli3*-*Gli1* regulatory axis. Together, our findings suggest that EED regulates the epigenetic state of specific genes in NSPCs to orchestrate cortical neurogenesis and cortical development.

RESULTS

Forebrain deletion of *Eed* leads to abnormal cortical architecture

By re-analyzing ENCODE RNA sequencing (RNA-seq) data of murine forebrains, we found that *Eed* was highly expressed in the embryonic brain from E11.5 to E15.5 (Figure S1A) and its mRNA expression level was gradually decreased during embryonic neocortex development (Figure S1B), suggesting that EED might play a pivotal role during embryonic cortical development. To specifically explore the role of EED, we generated the forebrain-specific *Eed* conditionally knockout mice (*Eed cKO*) by crossing $Eed^{fl/fl}$ mice with Emx1-Cre line (Figure S1C). RT-PCR and western blot analyses confirmed that EED expression was significantly decreased (Figures 1A and S1D), while a decreased H3K27me3 and an increased H3K27ac were observed in P21 *Eed cKO* cortical tissues (Figure 1B). *Eed cKO* mice were born at the expected Mendelian ratios and were indistinguishable from their wild-type (WT) littermates at birth. However, at the age of 3 weeks, *Eed cKO* mice became runted and brain weight decreased (Figures S1E–S1I). The survival curve showed that most *Eed cKO* mice died at P40 (Figure S1J). These results suggested that the deletion of *Eed* in the early embryonic forebrain leads to postnatal lethality and growth retardation.

During cortical development, the neocortex gradually expands its size and assembles into a six-layer structure from the inside to the outside (Tang et al., 2019). By comparing brain size, we found that cortical sizes were significantly decreased in *Eed cKO* compared with that of the WT littermates at E16.5 and P0 (Figure S2A). Next, we performed immunostaining of cortical layer-specific markers to assess the cortical structure at the cellular level. At E14.5, the numbers of TBR1+ and CTIP2+ deeper-layer (layers V–VI) neurons were markedly increased in the *Eed* cKO cortices (Figures 1C and 1D). Similarly, we also observed a significant increase of TUJ1+ cells in the E14.5 *Eed* cKO cortices (Figures S2B and S2C). However, there was no significant difference in the number of TBR1+ and CTIP2+ neurons at E16.5 and P0 (Figures 1C and 1D). Moreover, immunostaining of CUX1, SATB2, and BRN2 (layers II–IV) showed that the number of upper-layer neurons was significantly decreased in the *Eed* cKO cortices at E16.5 and P0 (Figures 1E–1H; Figures S2D and S2E). These observations suggested that EED might play an essential role in balancing the self-renewal and differentiation of cortical NSPCs during embryonic cortical development (Figure 1I).

Loss of EED decreases the pool of NSPCs

To determine whether the disorganization of the cortical layers in Eed-deficient mice was due to the depletion of the NSPCs, we performed immunostaining for PAX6 and TBR2 in cortices (Guillemot et al., 2006). Our results showed that there were no significant changes in the pool of NSPCs in the Eed cKO cortices at E12.5 (Figures 2A, 2B and 2E). However, the population of PAX6+ and TBR2+ cortical progenitor cells was both significantly decreased in E14.5 and E16.5 *Eed* cKO cortices (Figures 2A, 2B and 2E). Interestingly, our results showed that there was only a small population of ectopic PAX6+ cells, but not TBR2+ cells located at cortical plates in *Eed* cKO mice (Figures 2A and 2B). Taken together, our findings demonstrated that EED was required for the maintenance of the NSPCs pool in the late stages of embryonic neurogenesis.

Figure 1. EED is required for proper development of embryonic neocortex

(A) Representative images of western blot for EED, H3K27me3, and H3K27ac in P21 WT and *Eed* cKO cortices.

(B) Quantifications of EED and H3K27me3 protein expression levels in P21 cortices. EED, n = 4; H3K27me3 and H3k27ac, n = 3.

(C) Representative images of immunostaining of TBR1 and CTIP2 in E14.5, E16.5 and P0 WT and *Eed* cKO cortices. Scale bar, 50 μm.

(D) Quantifications of the number of deeper-layer (V–VI) neurons in E14.5, E16.5, and P0 cortices (n = 3 animals per group).

(E) Representative images of immunostaining of SATB2 and BRN2 in E16.5 WT and *Eed* cKO cortices. Scale bar, 50 μm.

(F) Quantifications of the number of upper-layer (II–IV) neurons in E16.5 WT and *Eed* cKO cortices (n = 3 per group).

(G) Representative images of upper-layer neuron marker CUX1 in P0 (WT, n = 3; *Eed* cKO, n = 3) WT and *Eed* cKO cortices.

(H) Bar graph shows the quantitative results of $Cux1^+$ cell numbers.

(I) Schematic diagram indicated deficits of *Eed* cKO in the development of embryonic neocortex. Data are presented as means ± standard error of the mean; two-tailed unpaired t-test; n.s., non-significant, *p < 0.05, **p < 0.01.

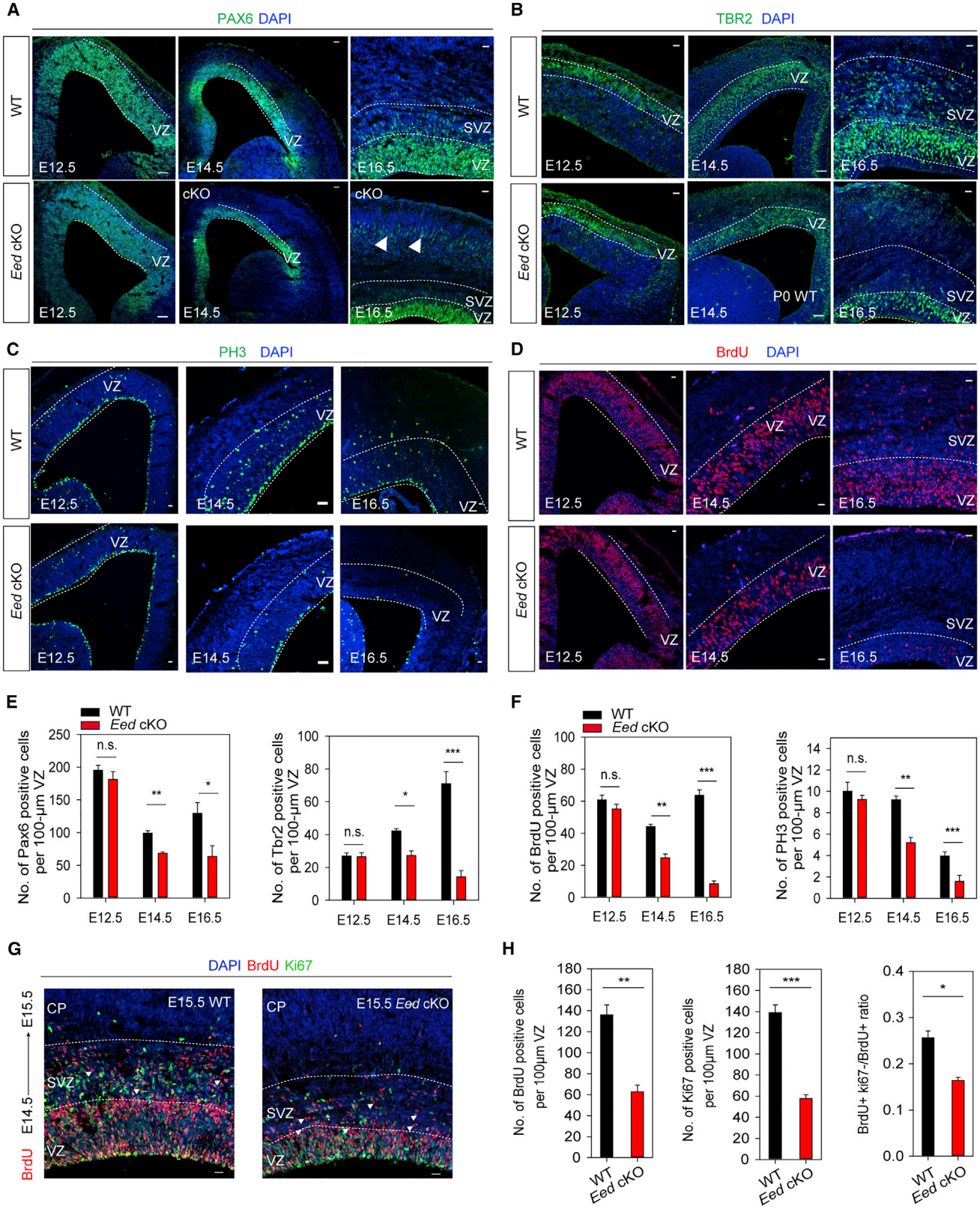

(legend on next page)

Loss of EED disrupts the balance between self-renewal and differentiation of NSPCs

To further investigate the intrinsic mechanism by which Eed loss of function decreased the pool of cortical NSPCs, we analyzed the proportion of proliferative cells in the S-phase in embryonic cortices after BrdU injection 2 h at different stages of pregnancy. Our results demonstrated that the number of BrdU+ cells was significantly decreased in both E14.5 and E16.5 *Eed cKO* mice cortices (Figures 2D and 2F) and P21 SVZ (Figure S3A), whereas the population of BrdU+ cells was unchanged in E12.5 *Eed cKO* mice (Figures 2D and 2F). In contrast with E14.5 cortices, BrdU+ cells almost completely disappeared in E16.5 *Eed cKO* mice ventricle zones (Figure 2D). Next, we used PH3 to examine the number of mitotic cells in the M-phase (Pearson et al., 2020). Consistent with the results of BrdU pulse labeling, the number of pH3+ cell was markedly decreased in E14.5 and E16.5 *Eed cKO* cortices (Figures 2C and 2F). Moreover, a neurosphere assay demonstrated that *Eed cKO* NSPCs formed fewer and smaller neurospheres than those from WT littermates at E13.5 (Figure S3B).

To examine whether the smaller number of PAX6+ and TBR2+ cells was caused by a decrease of cells exiting the cell cycle, we injected BrdU at E14.5 to label cycling progenitors and analyzed the fraction of BrdU+ cells 24 h later by co-staining with Ki67. The fraction of cells exiting the cell cycle (BrdU+/Ki67-fraction of BrdU+ cells) was significantly decreased in the VZs of *Eed cKO* mice (Figures 2G and 2H). We then cultured primary cortical NSPCs in a differentiated medium to assess their ability of neural differentiation, and we found that *Eed* depletion significantly increased the proportion of TUJ1+/DAPI+ cells in the *Eed cKO* group, suggesting that EED depletion promoted the differentiation of cortical NSPCs (Figure S3D). Collectively, these results suggested that the deletion of *Eed* in the developing forebrain imbalanced self-renewal and differentiation of NSPCs and decreased the number of NSPCs exiting the cell cycle in embryonic *Eed cKO* mice.

Eed deletion triggers massive apoptosis and DNA damage in NSPCs

To determine whether cell death occurred in the developing cortex after Eed deletion, we examined the number of cell apoptosis by immunostaining for cleaved-caspase3 and terminal deoxynucleotidyl transferase dUTP nick end-labeling (TUNEL). At E12.5, E14.5, and E16.5, we observed a larger number of apoptotic cells in *Eed cKO* cortices, compared with that of their WT littermates (Figures 3A and 3B). Of note, we found that almost all apoptotic cells were located in the VZ and SVZ regions at E12.5, E14.5, and E16.5 (Figures 3A and 3B). To determine whether apoptotic cells were RG cells or basal progenitors, we performed co-immunostaining for TUNEL, SOX2, and TBR2 and found that a large number of TUNEL+ cells were co-localized with SOX2+ cells, and a small amount of TUNEL+ cells co-localized with TBR2+ NSPCs (Figures S3E and S3F). During DNA replication, frequently stalled replication forks or free radicals can cause DNA breaks and DNA damage (Branzei and Foiani, 2010; Lee et al., 2012). Immunostaining for phosphorylated histone H2AX (γH2AX) displayed an increased accumulation of DNA damage in the VZ/SVZs of *Eed cKO* mice at E14.5 and E16.5 (Figures 3C and 3D). Together, these results suggested that *Eed* deletion leads to substantial apoptosis and increased DNA damage in the developing cortices, which might partially account for the decreased NSPC pool in embryonic *Eed cKO* mice.

EED regulates a specific transcription program for cortical neurogenesis

During cortical neurogenesis, cortical neurons at the E14.5 stage mainly originate from neural stem cells at the E12.5 stage (Agirman et al., 2017; Yoon et al., 2017). To further dissect the regulatory mechanism of EED in early cortical neurogenesis, we performed an RNA-seq analysis of forebrain tissues collected from both WT and *Eed cKO* littermates at E12.5. Deletion of *Eed* resulted in highly reproducible changes in the transcriptome, and 674 genes ($p < 0.05$) showed significant changes (Figure 4A). The clustering analysis and PCA showed a clear discrimination between the *Eed cKO* and WT (Figures S4A–S4C), indicating that EED regulated distinct transcription programs. A volcano plot showed that 420 genes were down-regulated and 254 genes were up-regulated in E12.5 *Eed cKO* forebrain (Figure 4A). A gene ontology (GO) analysis showed that the down-regulated

Figure 2. EED regulates the proliferation and cell cycle exit of cortical progenitor cells

(A–D) Representative images of E12.5, E14.5, and E16.5 cortices stained for PAX6 (neural stem/progenitor marker), TBR2 (basal progenitor marker), pH3 (mitosis marker), and BrdU. White arrow heads indicated the abnormal location of $PAX6^+$ cells. VZ, ventricle zone. Scale bar, 50 μm.

(E, F) Quantitative analysis of the number of PAX6, TBR2, pH3, and BrdU in E12.5, E14.5, and E16.5 WT and *Eed* cKO cortices (n = 3–4 mice per group).

(G) Representative images of E15.5 cortices stained for of Ki67 and BrdU after BrdU treatment 24 h. Arrowheads indicated $BrdU^+/Ki67^-$ cells. Dashed white lines indicated the border of VZ or SVZ. VZ, ventricle zone. Scar bar, 50 μm.

(H) Quantitative analysis of the number of $BrdU^+$ or $Ki67^+$ NSPCs in E15.5 WT and *Eed* cKO cortices (n = 3 mice per group). Data are presented as means ± standard error of the mean; two-tailed unpaired t-test; n.s., non-significant, $^*p < 0.05$, $^{**}p < 0.01$, $^{***}p < 0.001$.

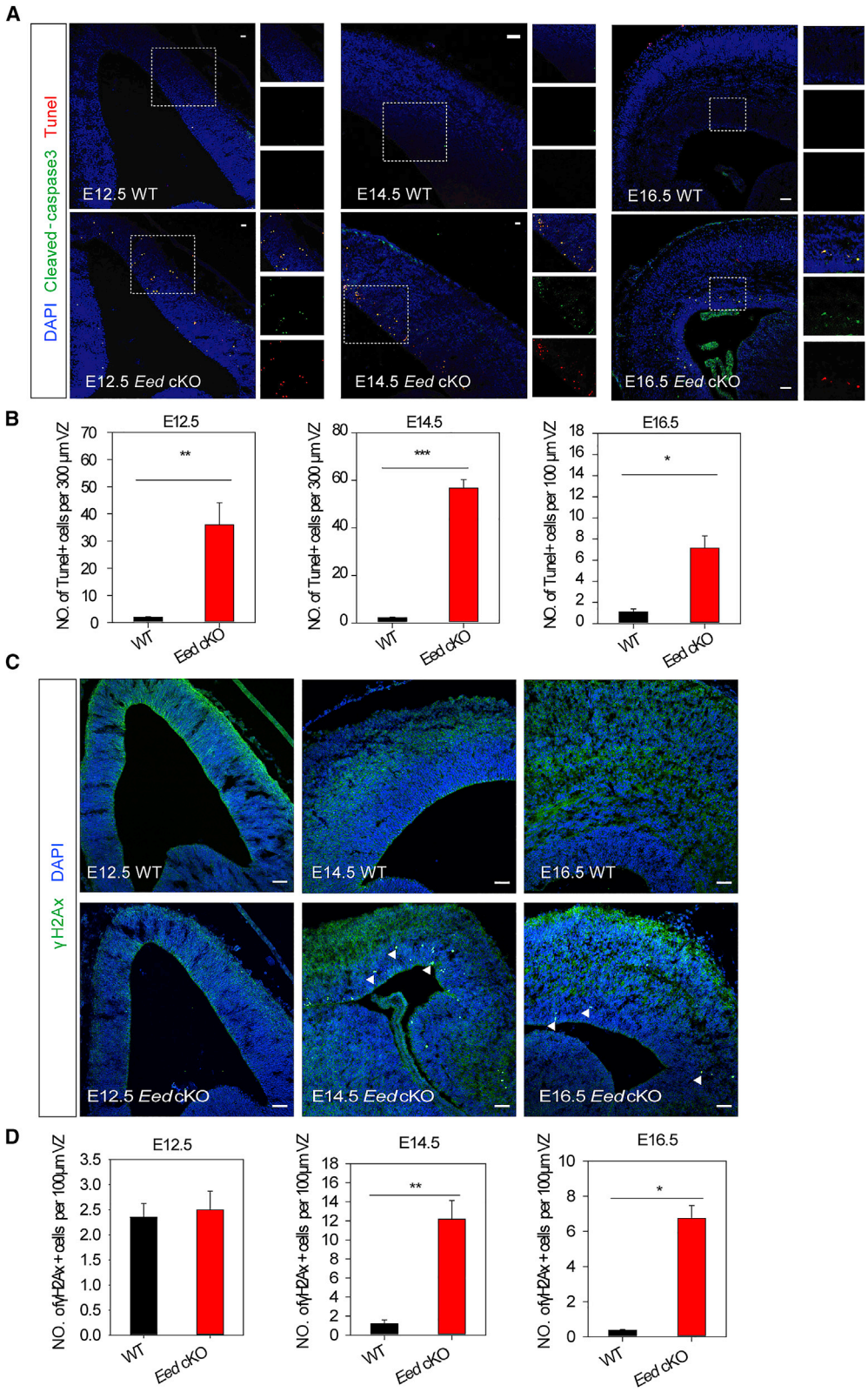

(legend on next page)

genes were significantly enriched for several cellular biological processes, including cerebral cortex development, forebrain development, positive regulation of neural precursor cell proliferation, and layer formation in cerebral cortex (Figure 4B). In contrast, the up-regulated genes were enriched for forebrain development, telencephalon development, negative regulation of neurogenesis, and G2/M transition of mitotic cell cycle (Figure 4C). Notably, a Kyoto Encyclopedia of Genes and Genomes (KEGG) analysis further indicated that differentially expressed genes were significantly enriched for Hedgehog signaling pathway, cyclic AMP (cAMP) signaling pathway, and hippo signaling pathway (Figures 4D, 4E and S4D), which regulate developmental processes including cortical development (Belgacem et al., 2016; Cayuso et al., 2006; Komada et al., 2008, 2013; Lavado et al., 2018).

Next, to explore whether EED directly regulates the dysregulated genes, we performed chromatin immunoprecipitation followed by chromatin immunoprecipitation sequencing (ChIP-seq) for EED and CUT&Tag-seq for RNA-Pol2, H3K27me3, and H3K27ac in WT and *Eed cKO* forebrains at E12.5, when the majority of NSPCs give rise to E14.5 upper-layer neurons. We detected 34,518 EED peaks (false discovery rate <0.01). To validate the specificity of these binding sites, we compared the normalized EED-binding levels (RPKM) on promoter regions (±1 Kb) between E12.5 WT and *Eed cKO* forebrains (Figure 5C). The majority of EED-binding sites (75%) were located at the promoter regions (0–3 Kb) (Figure 4F). Motif analysis of EED-binding promoter sequences (±3 Kb) indicated that EED shares several common motifs with neural development related genes, including Wt1 (Ji et al., 2021), E2F3 (Julian et al., 2013), and Ascl2 (Liu et al., 2019b) (Figure 4G). Meanwhile, a lot of homeobox family genes (such as Hoxd12, Hoxa13, and Lhx3), known as PRC2 targets, were also identified (Figure 4G) (Conway et al., 2015).

Furthermore, we used a BETA analysis (Wang et al., 2013), an integrative analysis of RNA-seq data and ChIP-seq data, to identify the potential direct targets of EED. In BETA analysis, both fold changes of gene expression in RNA-seq and the number and proximity of EED-binding sites to the TSSs were used to predict the most potential target genes of EED (Figures 4H and 4I). Surprisingly, our results suggested that EED might act as a repressor (p = 1.25e-7) as well as an activator (p = 4.46e-12) (Figure 4H). The top 60 up-regulated potential targets and 115 down-regulated potential targets of EED (Figure 4I) were significantly enriched for forebrain development, and positive regulation of neuron differentiation (Figures 4J and S4E). Several neural differentiation-associated genes, such as *Neurod2*, *Neuog1*, and *Fezf2*, were displayed in the IGV genome browser, suggesting that these genes were targeted by EED (Figure S4G). Importantly, a KEGG analysis of 175 predicted targets showed that the Hedgehog signaling genes were significantly altered after *Eed* deletion (Figure S4F). Collectively, our results suggest that EED regulates a specific transcription program for cortical neurogenesis and forebrain development.

The absence of EED alters the epigenetic modification state on the *Gli3* promoter

Our western blot results showed that H3K27me3 and H3K27ac modification levels were significantly changed in *Eed* cKO forebrains (Figure 1B). To explore the underlying mechanism of gene expression subjected to epigenetic changes, we assessed the H3K27me3, H3K27ac, and RNA-Pol2 binding levels on EED-binding sites in E12.5 WT forebrains. Meta-analysis showed high H3K27me3 abundance at EED binding sites (±5 Kb) (Figures 5A and 5B). However, relatively lower binding levels of H3K27ac and RNA-Pol2 were observed on the EED-binding sites (±5 Kb) (Figures 5A and 5B). At the whole genome level, a significant decrease in EED- and H3K27me3-binding levels at transcription start sites (TSSs) (±3 Kb) was detected in E12.5 *Eed* cKO forebrains (Figures 5C–5E). However, the binding levels of H3K27ac and RNA-Pol2 significantly increased within TSSs (±3 Kb) (Figures 5D and 5E). To further explore the relationship between an EED-regulated epigenetic state and EED-regulated gene expression patterns, we combined differential expression genes of RNA-seq and the annotated differential binding genes of ChIP-seq and CUT&tag in the E12.5 forebrain. Venn diagram showed that there were 56 common genes among the EED_loss gene set, H3K27me3_gain gene set, H3K27ac_gain gene set, and RNA up-regulated gene set. A GO enrichment analysis ($p < 0.00001$) of these common genes suggested their functions in neural development, neurogenesis, and neuron differentiation (Figures 5F and 5G). A KEGG analysis identified 5 of 56 common genes (*Gli3*, *Gli2*, *Gas1*, *Ccnd2*, and *Cdon*) belonging to the Hedgehog signaling pathway (Figure 5H). Overlap analysis of these 56 genes with EED potential up-regulated targets and murine factors (download from TRRUST database, https://www.grnpedia.org/trrust/) found that GLI3 was the only factor that was

Figure 3. *Eed* deletion triggers massive cell apoptosis and DNA damage

(A) Representative images of E12.5, E14.5, and E16.5 WT and *Eed* cKO cortices stained for cleaved-caspase3 and TUNEL. Scale bars, 50 μm.

(B) Quantification of TUNEL+ apoptotic cells in WT and *Eed* cKO cortices at the indicated timepoints (n = 3–4 animals per group).

(C) Representative images of E12.5, E14.5, and E16.5 WT and *Eed* cKO cortices stained for γH2AX. Scale bar, 50 μm.

(D) Quantification of γH2AX + cell numbers in *Eed* WT and cKO cortices at the indicated timepoints (n = 3–4 animals per group). Data are presented as means ± standard error of the mean; two-tailed unpaired t-test; *p < 0.05, **p < 0.01.

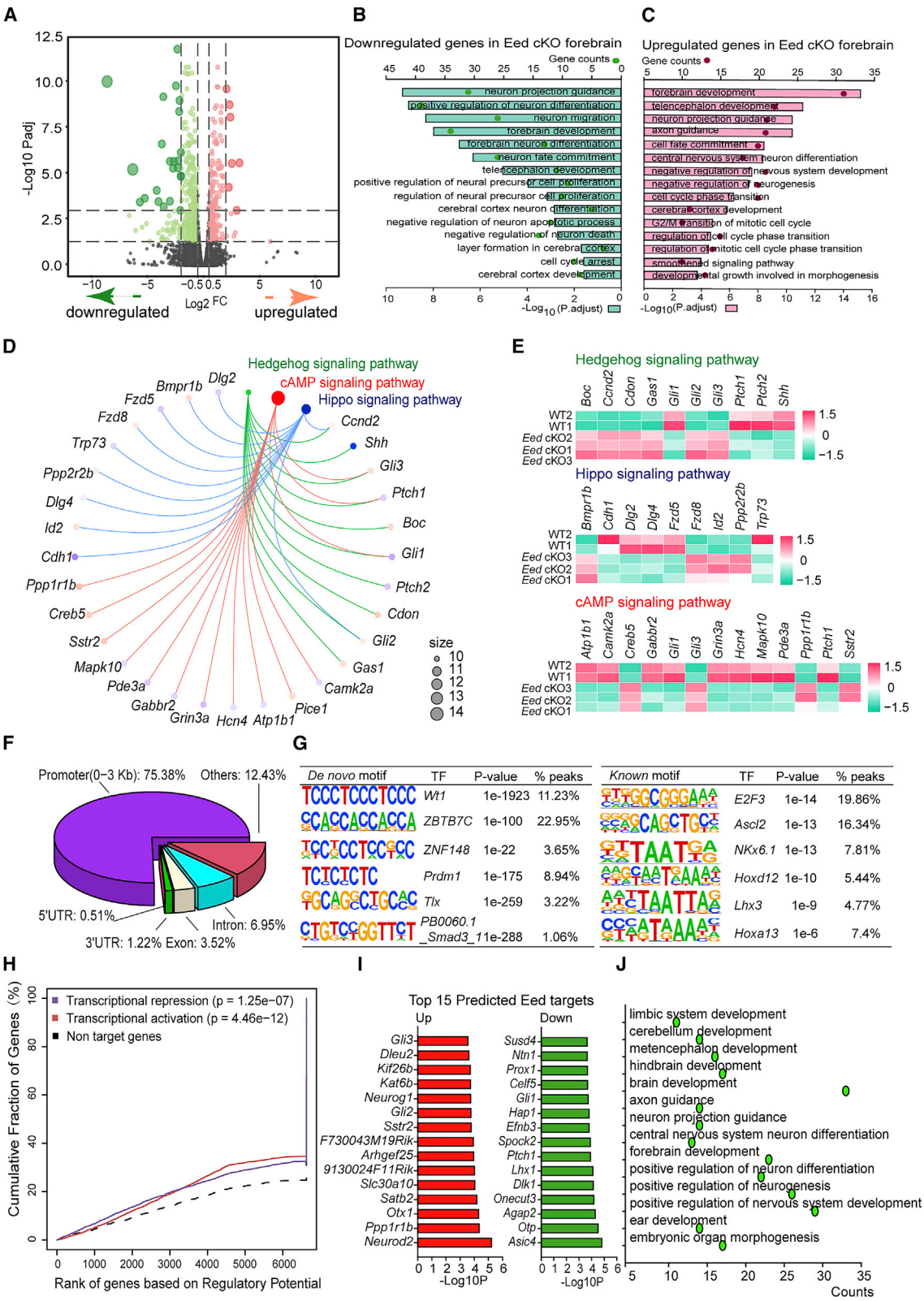

(legend on next page)

the most likely potential downstream target of EED (Figure 5I). Indeed, IGV visualization of the *Gli3* loci showed a significant decrease in EED- and H3K27me3-binding levels and a significant increase in H3K27ac- and RNA-pol2-binding levels within *Gli3* TSS (Figures 5J and S5A). Together, these findings suggested that EED regulated the epigenetic state of *Gli3*, and that *Gli3* may be the key downstream target of EED in regulating cortical neurogenesis.

GLI3 acts as a key repressor of Hedgehog signaling in the developing forebrain

To compare the dynamic expression of Gli3 during cortical development, *in situ* hybridization data of *GLI3* were downloaded from the ALLEN BRAIN ATLAS. As expected, *Gli3* mRNA was highly expressed in the ventricle zones of the developing forebrain (Figure S5E). To validate the Gli3 expression levels in the developing forebrain, we re-analyzed publicly available murine forebrain RNA-seq data and found that the expression level of *Gli3* mRNA was gradually decreased during development (Figure S5F). Notably, our RT-PCR analysis verified a significant increase in Gli3 expression as well as a significant decrease in Gli1 expression in E12.5 *Eed cKO* cortices (Figure S5B). Consistently, western blot analyses showed that both GLI3 full-length (Gli3FL, 190 KDa) and GLI3 repressor (Gli3R, 89 KDa) fragments were significantly increased in E15.5 *Eed cKO* cortices (Figure 6A). Meanwhile, markedly decreased GLI1 protein was detected in E15.5 *Eed cKO* cortex tissues compared with that of WT littermates (Figure 6B). Interestingly, we observed simultaneously decreased GLI1 and increased GLI3 expression (Figures 6A, 6B and S5B). A previous study reported that an increased *Gli3* expression can repress the Hedgehog signaling pathway in acute myeloid leukemia (Chaudhry et al., 2017). To determine whether the reduced *Gli1* was attributable to an increased *Gli3* in the *Eed* cKO forebrain, we applied a small interfering RNA (siRNA) and an overexpression plasmid to manipulate *Gli3* expression in NE-4C cells, a neural stem cell-like cell line derived from embryonic neuroepithelial cells (Aprea et al., 2013; Li and Jiao, 2017). Knockdown of *GLI3* led to a significant decrease of Gli3F and Gli3R and a significant increase of GLI1 protein expression (Figure 6C). Consistently, overexpression of GLI3 significantly increased Gli3F and Gli3R, whereas GLI1 expression was significantly decreased (Figure 6D). Thus, our observations demonstrate a regulatory relationship between GLI3 and *Gli1* in NSPCs, suggesting that GLI3 was a crucial repressor of Hedgehog signaling in the developing cortex.

Gli3 regulates proliferation of cortical progenitors via repressing Hedgehog signaling

To analyze the expression levels of *Gli3* and *Gli1* in the developing cortex, we re-analyzed publicly available E14.5 RNA-seq data in proliferative progenitors, differentiating progenitors, and neurons (Aprea et al., 2013). We found that both *Gli3* and *Gli1* were highly expressed in neural progenitor cells, but not in neurons (Figures S5C and S5D). Our immunofluorescence staining showed that GLI1 was highly expressed in early cortical progenitor cells (Figure 6G). Given that EED suppresses Hedgehog signaling, we next asked whether the re-activation of Hedgehog signaling could rescue the phenotypes caused by *Eed* deletion. To test this idea, we used a specific Smo activator SAG (Bragina et al., 2010; Wu et al., 2017) to activate Hedgehog signaling activity in E13.5-derived NSPCs. BrdU incorporation showed that activation of Hedgehog signaling pathway *in vitro* could rescue the proliferation defects of *Eed cKO* cortical progenitors (Figures 6H and 6I), suggesting that the Hedgehog signaling played an essential role in EED-deficient cortical neurogenesis. Given that GLI3 is a repressor of Hedgehog signaling (Figures 6C and 6D), we hypothesized that decreased GLI3 expression could eliminate the defects of cortical progenitor cells caused by Eed depletion. To test this hypothesis, we used *Gli3*-specific siRNAs to inactivate *Gli3* in E13.5-derived NSPCs. Notably, repression of *Gli3* expression by siRNAs could rescue the proliferation defects in E13.5 *Eed cKO* NSPCs *in vitro* (Figures 6E and 6F). Collectively, our findings

Figure 4. Transcriptome sequencing and genome occupancy analysis in E12.5 WT and *Eed* cKO forebrain

(A) Volcano plot shows 420 down-regulated genes (green) and 254 up-regulated genes (orange) in E12.5 *Eed* cKO forebrains. WT, n = 2; *Eed* cKO, n = 3.

(B, C) Bar charts depicting the top GO terms (p-adjust < 0.05) of down-regulated genes and up-regulated genes in E12.5 *Eed* cKO forebrains.

(D) The KEGG pathway analysis of differential expression genes in E12.5 *Eed* cKO forebrains.

(E) Heatmaps show dysregulated genes were enriched in the cAMP signaling, Hippo signaling, and Hedgehog signaling pathways.

(F) Pie chart illustrating the distribution of EED binding sites in the genome at E12.5.

(G) Sequence logos corresponding to top enriched motifs within EED-binding sites identified by *de novo* motif analysis.

(H) Statistical integration analysis of dysregulated genes in E12.5 *Eed* cKO forebrains predicted a dual function of EED as an al repressor (blue line) and an activator (red line), using a reference set of non-differentially expressed genes (dashed black line) for normalization. The p values for each function were indicated in the chart.

(I) Top predicted al targets of EED in E12.5 forebrains.

(J) Bar plots showing the top GO terms (p-adjust < 0.05) of top 200 up-regulated and 200 down-regulated targets of EED.

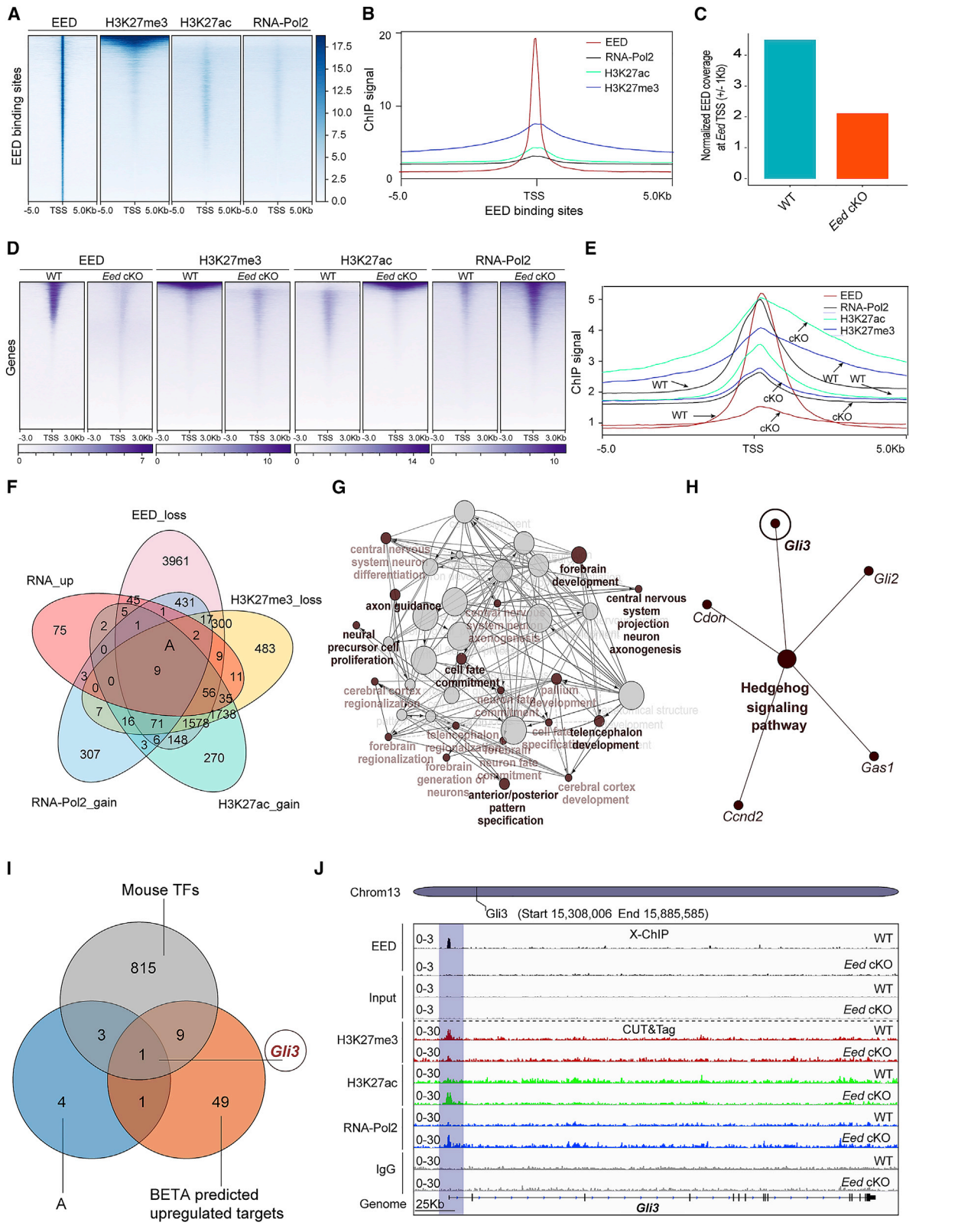

(legend on next page)

demonstrated that EED activated the Hedgehog signaling pathway by repressing Gli3 during cortical neurogenesis.

Activation of Hedgehog signaling partially rescues aberrant cortical neurogenesis caused by *Eed* deletion

To verify that EED regulates cortical neurogenesis via the EED-Gli3-Gli1 regulatory axis *in vivo*, we performed intraperitoneal injection of SAG in pregnant mice from E9.5 to E15.5 and analyzed mouse embryonic brains at E16.5 (Figure 7C). First, to determine whether the treatment of SAG could activate Hedgehog signaling *in vivo*, we assessed GLI1 protein expression after treatment of 5 mg/kg SAG from E13.5 to E15.5 (Figure 7C). A western blot analysis demonstrated that treatment of SAG could rescue the Gli1 protein level (Figure 7B). Next, we evaluated the changes in cortical size after administration of SAG. Compared with the control group, treatment of SAG could rescue the defects of projected cortical area caused by EED disruption (Figure 7D). Furthermore, we examined the cortical lamination structure by immunostaining for upper-layer marker SATB2 and deeper-layer marker TBR1 and CTIP2, respectively. Treatment of SAG could partially rescue the defects of decreased upper-layer neurons (Figure 7E), but not of the deeper-layer neuron population (Figures S6A and S6B). In addition, we performed immunostaining for PAX6 and TBR2 to examine the population of cortical progenitor pool (RG cells and IPs). We did not observe any significant change in the Pax6+ cell population in SAG-treated group (Figures S6E and S6F), whereas the defect of a decreased TBR2+ cell number in E16.5 *Eed cKO* cortex was partially rescued by treatment of SAG (Figures S6G and S6H). Of note, the treatment of SAG could partially rescue apoptosis in EED deletion cortices (Figures S6C and S6D). This is consistent with a previous report showing that SMO knockout, increased apoptosis of cortical progenitor cells (Komada et al., 2008). Finally, we assessed cortical progenitor cell proliferation and found that treatment of SAG could partially rescue the defects of cortical progenitor cell proliferation in *Eed* cKO cortex (Figure 7G). Together, these results demonstrated that pharmacological re-activation of Hedgehog signaling partially rescued the EED deficiency-induced neural phenotypes during cortical neurogenesis.

To further determine the function of the Hedgehog signaling in the cortical development, we performed genetic activation. We obtained *Ptch1* and *Eed* double conditional knockout (*Eed*/*Ptch1* dcKO) mice by $Ptch1^{f/f}$ and $Eed^{f/f}$ mice, which were crossed with *Emx1-Cre* mice. We first examined the cortical size by quantification of the projected cortical area in WT, *Eed* cKO, *Ptch1* cKO, and *Eed/Ptch1* dcKO mice. Our results showed that the decreased sizes of the projected cortical area in E16.5 *Eed* cKO mice could be rescued by inactivation of *Ptch1* (Figure 7F). Next, to determine whether the defects in the cortical progenitor cell pool caused by *Eed* deletion could be rescued or not, we performed immunostaining for PAX6 and TUJ1. Although PAX6+ cells in *Ptch1* cKO and *Eed/Ptch1* dcKO cortices displayed diffuse distribution, the numbers of PAX6+ and TUJ1 cells were significantly increased in *Ptch1* cKO or *Eed/Ptch1* dcKO cortices. Compared with *Ptch1* cKO mice, *Eed/Ptch1* dcKO mice displayed a slightly reduced number of PAX6+ and TUJ1+ cells (Figure 7H), suggesting that the re-activation of Hedgehog signaling could partially rescue the defects of cortical neurogenesis. Taken together, our results provided multiple lines of *in vitro* and *in vivo* evidence demonstrating that EED orchestrated cortical neurogenesis through *Gli3*-mediated suppression of the Hedgehog signaling in the developing forebrain.

DISCUSSION

Here, we reveal the EED-*Gli3*-*Gli1* regulatory axis in maintaining the NSPCs pool for cortical neurogenesis. Mechanistically, EED modifies the epigenetic switch of H3K27me3/H3K27ac marks at the TSS of key genes during

Figure 5. Loss of EED alters the epigenetic state on the *Gli3* promoter

(A) Heatmaps display enrichments for EED, H3K27me3, H3K27ac, and RNA-Pol2 within EED-binding promoters (±5 Kb) in E12.5 WT forebrain. WT, n = 1; *Eed* cKO, n = 1.

(B) Plots of average enrichment profiles within ±5 Kb promoter regions of annotated EED-binding genes for EED, H3K27me3, H3K27ac, and RNA-Pol2.

(C) Bar chart indicates normalized EED-binding levels within the genome promoter regions in E12.5 WT and *Eed* cKO forebrains.

(D) Heatmaps shows enrichment for EED, H3K27me3, H3K27ac, and RNA-Pol2 within ±3 Kb promoter regions of all GENCODE annotated genes.

(E) Plots of average enrichment profiles within ±3 Kb promoter regions of all GENCODE annotated genes.

(F) Venn diagram of a combined comparison between differentially expressed genes and differentially binding genes.

(G) Network diagram indicates enriched GO terms ($p < 0.0001$) in a combined gene set (56 genes, with decreased EED binding, decreased H3K27me3 binding, increased H3K27ac binding, and RNA-seq up-regulated).

(H) The network diagram exhibits Hedgehog pathway genes, which are enriched by KEGG from the same gene set in (G).

(I) Venn diagram of a combined comparison between gene set "A" (generated in {), top 200 potential targets, and 828 mouse factors.

(J) Genome browser views of ChIP-Seq and CUT&Tag-seq data at the *Gli3* loci in the Integrative Genomics Viewer (IGV). Scale bars, 25 Kb.

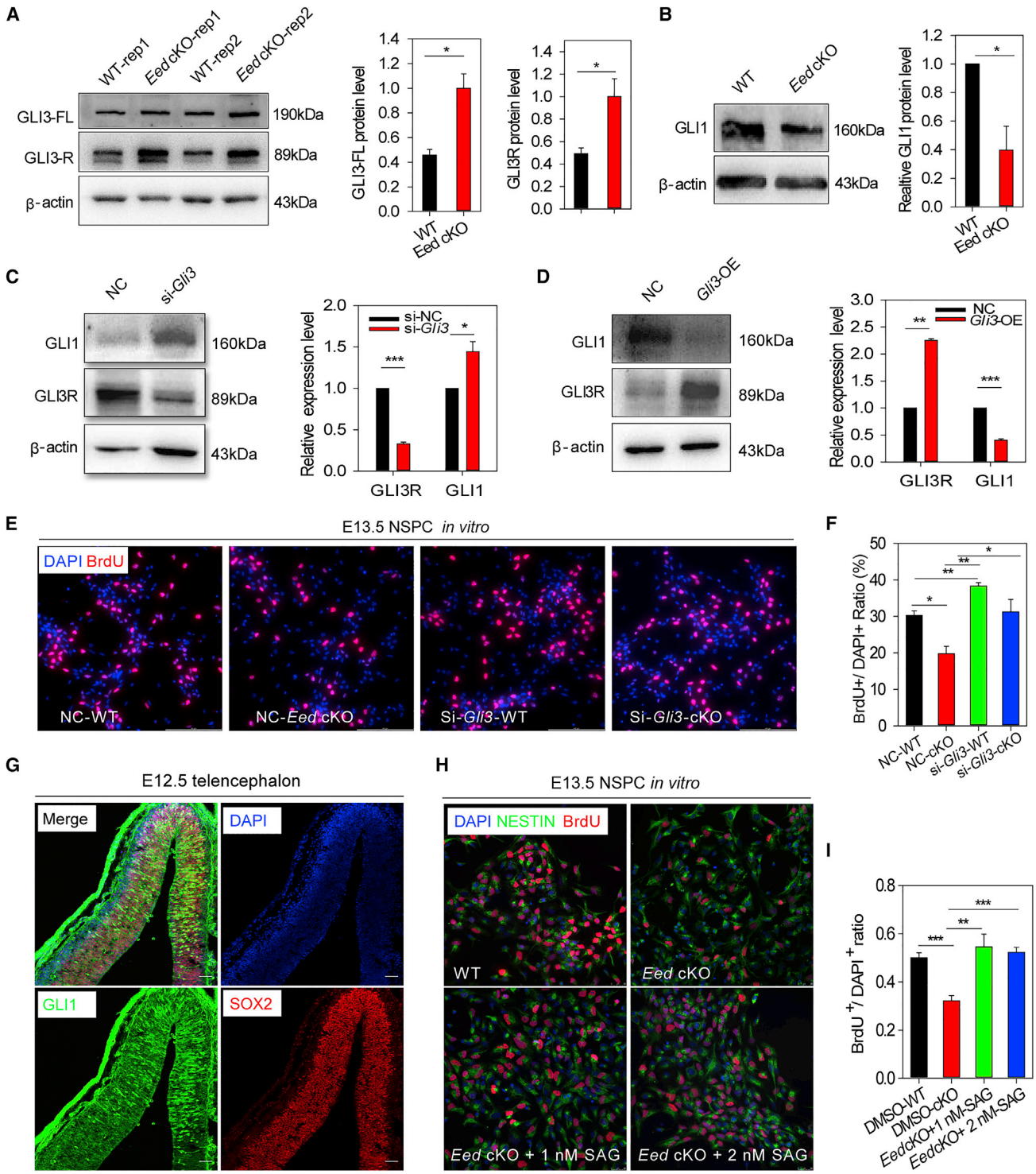

Figure 6. Knocking down of GLI3R promotes the proliferation of NSPCs *in vitro*

(A) Representative images and quantification of western blot for GLI3-FL (full-length) and GLI3-R (repressor) in E15.5 *Eed* cKO and WT forebrains. n = 3 mice per group.

(B) Representative images and quantification of western blot for GLI1 in E15.5 *Eed* cKO and WT forebrains. n = 3 mice per group.

(C) western blot analysis shows a significant reduction of GLI3R and a significant increase of GLI3 in NE4C cells after treated with 20 nM *Gli3* small interfering RNA (siRNA) for 48 h (n = 3 independent experiments).

(legend continued on next page)

cortical neurogenesis. Ablation of *Eed* in the embryonic forebrain altered the H3K27me3/H3K27ac ratio on differentiation-promoting genes, leading to enhancement of the recruitment of RNA-Pol2 and up-regulation of gene expression. As a result, this causes an acceleration of the neuronal differentiation programs and depletion of NSPCs pool. On the other hand, loss of EED blocked the self-renewal of NSPCs and attenuated the production of embryonic neural/stem progenitor cell pool (Figure S7). Loss of EED increased the neuronal population at E14.5, but specifically decreased the upper-layer neuron population at a late stage of cortical neurogenesis. We believe that the accelerated depletion of NSPCs pool is mainly responsible for the decrease in neurons at the middle and late stages of neurogenesis. In the early stage of cortical neurogenesis, only a small number of NSPCs differentiate into neurons, and cell pool is sufficient at this time. However, as neurogenesis reaches its peak, the deficits in NSPCs pool caused by EED deletion become apparent (Figures S7D and S7E). Therefore, we propose EED as an essential "speed bump" during neurogenesis by maintaining the appropriate speed of neurogenesis (Figure S7E).

Recent clinical studies indicate that multiple forms of *EED* mutations in humans can cause Weaver syndrome, a neural developmental disorder (Cohen and Gibson, 2016; Cohen et al., 2015; Smigiel et al., 2018; Spellicy et al., 2019). Clinically, isolated ventriculomegaly is a common symptom in Weaver syndrome (Al-Salem et al., 2013; Tatton-Brown et al., 2013). In our study, we observed a significantly decreased cortical size in postnatal *Eed* cKO mice, which is inconsistent with megalencephaly seen in patients with missense mutations (Gibson et al., 2012). Our genome occupancy analysis showed that EED shared several common motifs with many factors that regulate neurodevelopment, suggesting that *Eed* truncating mutations may lead to distinct phenotypes as compared with missense mutations. Therefore, we speculate that distinct mutation patterns may account for the different phenotypes between mice and humans. Previous studies suggest that EED is essential for postnatal neural stem cell proliferation (Liu et al., 2019a; Sun et al., 2018). Compared with *Ezh2* mutant mice (Pereira et al., 2010), we observed defects in both the proliferation and differentiation of NSPCs, as well as unique phenotypes in early stage of *Eed*-mutant mice. Our findings suggest that EED may have PRC2-independent regulatory mechanisms during cortical development.

In the developing human cortex, SHH is widely expressed in neural progenitors and neurons in the dorsal cortex (Memi et al., 2018). Similarly, we found that SHH is also highly expressed in neural progenitor cells on the apical surface of the ventricle and neurons (Figures S5G–S5I). Previous studies have shown that the Hedgehog signaling is crucial for neural development and cortical neurogenesis (Komada et al., 2008, 2013; Wang et al., 2016a). Forebrain-specific conditional knockout of SMO and SHH lead to serious defects, including a smaller size of dorsal telencephalon, suppressed proliferation of cortical progenitor cells, and increased apoptosis of cortical progenitor cells. Moreover, dysfunction of Hedgehog signaling causes holoprosencephaly, a defect in the separation of the brain hemispheres that is often derived from abnormal patterning (Derwinska et al., 2009; Stashinko et al., 2004; Wang et al., 2016b). In the current study, our findings in *Eed*-ablated mice are consistent with the phenotypes observed in *Smo* and *Shh* mutants, two major members of the Hedgehog signaling pathway (Komada et al., 2008). Importantly, SAG, a small molecule activator targeting SMO, could partially rescue the cortical development defects caused by *Eed* deletion. Therefore, it strongly supports the notion that EED regulates cortical development through the *EED-Gli3-Gli1* regulatory axis.

NSPCs are subjected to strictly spatiotemporal regulation of both intrinsic and extrinsic factors (Li et al., 2019; Paridaen and Huttner, 2014). In our study, we found that the deletion of *Eed* altered the expression of Hippo signaling and cAMP signaling pathway genes. However, we cannot exclude the possibility that other pathways may regulate cortical neurogenesis to a certain extent. Indeed, by using multiple different strategies, re-activation of the Hedgehog pathway cannot fully rescue the cortical development defects caused by *Eed* loss of function. Whether and how other pathways regulate cortical neurogenesis warrants further investigations.

(D) Western blot analysis of GLI3R protein level and GLI1 protein level in NE4C cells transduced with 3 μg Gli3-overexpression plasmid for 48 h (n = 3 independent experiments).
(E) Representative images of BrdU staining of NSPCs (isolated from E13.5 forebrains), which were treated with PBS, 1 nM SAG or 2 nM SAG in a proliferation medium and cultured for 48 h. After treatment, 20 μM BrdU was added for 6 h to examine the proliferation of NSPCs.
(F) Quantitative results of (E).
(G) Representative images of E13.5 WT brain sections stained for GLI1 and SOX2. Scale bars, 50 μm.
(H) Representative images of NESTIN and BrdU immunostaining of primary cultured E13.5 NSPCs transfected with negative control siRNA or *Gli3* siRNA for 48 h in proliferation medium.
(I) Quantitative results of (H). Data are presented as means ± standard error of the mean; two-tailed unpaired t-test, n.s., non-significant, *p < 0.05, **p < 0.01, ***p < 0.001.

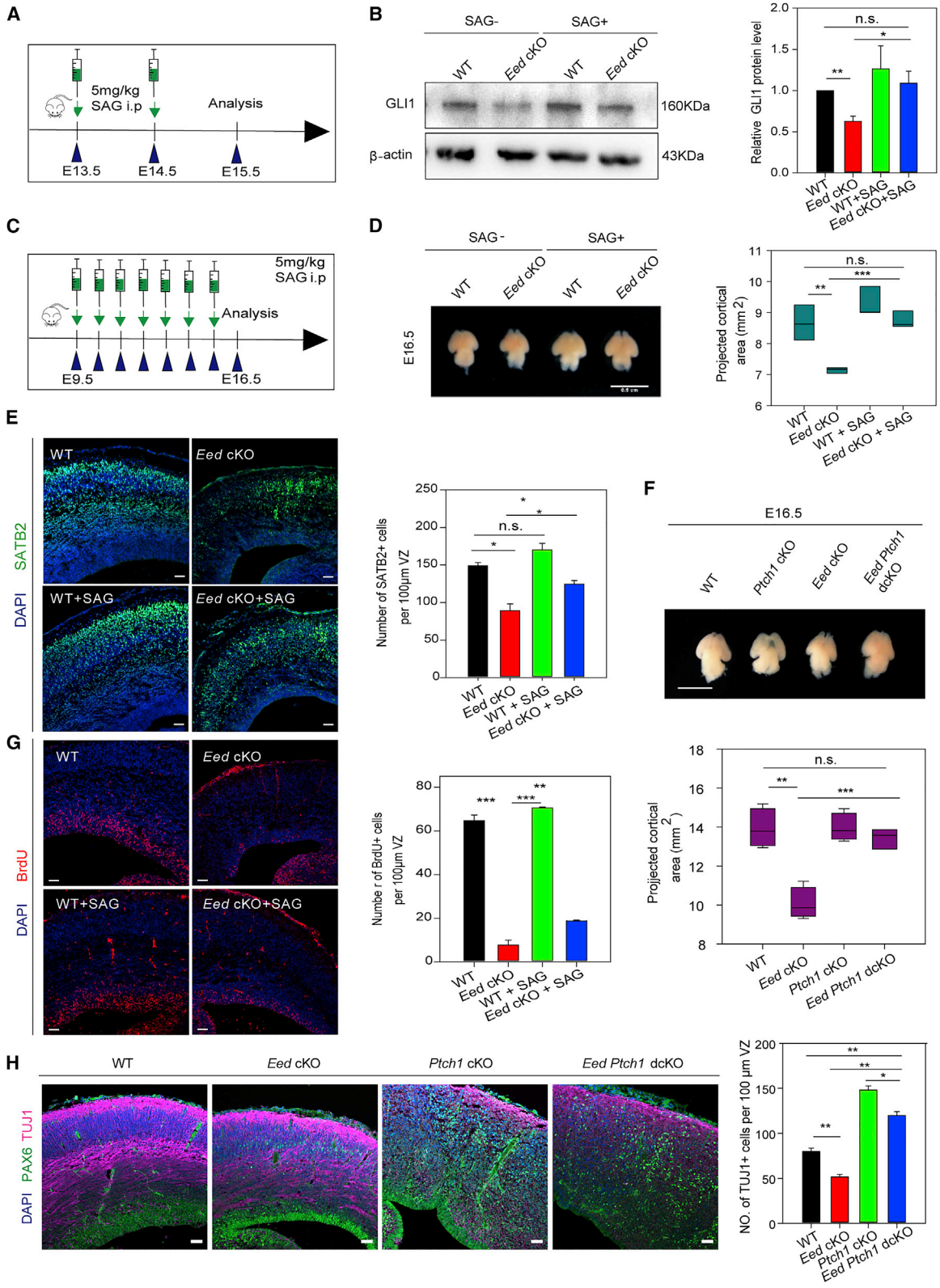

(legend on next page)

EED has been considered indispensable for the H3K27me3 mark (Boyer et al., 2006; Margueron and Reinberg, 2011). Traditionally, EED is thought to act as a transcriptional repressor by establishing the repressive mark H3K27me3 (Margueron et al., 2009). In our study, we found that *Eed* deletion can significantly decrease H3K27me3, but increase H3K27ac marks. Additionally, transcriptome analysis shows that there are a number of down-regulated genes upon *Eed* ablation. We speculate that there are other mechanisms by which EED regulates transcriptional programs in the developing cortex. Moreover, we found that EED-bound genes were not necessarily enriched for H3K27me3 in the WT mouse forebrain (E12.5), suggesting that EED may regulate gene expression independent of the enzymatic activity of the PRC2 complex. Of note, EED shares several common motifs with many transcription factors related to neurodevelopment, which further indicates that EED may be a versatile regulator. The contribution of accurate EED regulated mechanisms during cortical neurogenesis needs further experimental investigations.

Taken together, our results identify a novel EED-*Gli3*-*Gli1* regulatory axis in the developing cortex, which may provide a better understanding of the pathogenesis of neurodevelopmental disorders. Given the emerging evidence linking PRC2/EED to neurological diseases, our study not only sheds novel mechanistic insight into the genetic basis of EED in neural development disorders, but also facilitates further investigation of potential intervention strategies for neurodevelopmental defects.

EXPERIMENTAL PROCEDURES

Detailed descriptions of experimental procedures can be found in the Supplemental information.

Animals

All mice used in the current study have a C57BL6 background. All mouse experiments were approved by the Animal Committee of the Institute of Zoology, Chinese Academy of Sciences, Beijing, China. The genotyping primer for mutant mice in Supplemental Experimental Procedures.

Proliferation, differentiation, and self-renewal analysis of cultured NSPCs

Isolation and culture of the primary NSPCs, proliferation, differentiation and self-renewal of NSPCs assays were performed as previously described (Liu et al., 2017, 2019a) in detail in the Supplemental Experimental Procedures.

Immunostaining

Immunofluorescence was performed as described previously (Liu et al., 2017, 2019a). Briefly, the embryonic brains were cut into 15-μm-thick sections and mounted on Superfrost Plus microscope slides. Sections were incubated with primary antibodies in the 2% BSA and 0.5%Triton X-100 at 4°C overnight. Secondary antibodies were incubated in the 2% BSA and 0.5%Triton X-100 at room temperature for 2 h. High magnification fluorescent images were acquired using a Zeiss LSM 780 or LSM 880 confocal microscope. For more details, please see the Supplemental Experimental Procedures.

Western blot and RT-PCR

Samples were prepared and analyzed as described in detail in the Supplemental Experimental Procedures.

Data availability

RNA-seq, ChIP-seq, and CUT&tag data associated with this manuscript can be found at the GEO repository under the accession number GSE169653.

SUPPLEMENTAL INFORMATION

Supplemental information can be found online at https://doi.org/10.1016/j.stemcr.2022.07.004.

AUTHOR CONTRIBUTIONS

Conceptualization: C.M.L., S.F.Z; Design and analysis of experiments: S.F.Z, S.K.D, H.Z.D, H.W.; Writing - original Draft: S.F.Z;

Figure 7. Activation of Hedgehog signaling pathway partially rescues aberrant cortical neurogenesis

(A) Schematic diagram of the treatment of 5 mg/kg SAG from E13.5 to E14.5.

(B) After the treatment of SAG from E13.5 to E14.5, quantification of western blot of GLI1 expression level in E15.5 *Eed* cKO cortices. n = 3 mice per group.

(C) Schematic diagram of treatment of 5 mg/kg SAG from E9.5 to E15.5. n = 3 mice per group.

(D) Representative images and quantification of the projected cortical areas of E16.5 *Eed* cKO and WT mice.

(E) Represent images and quantification of the number of $SATB2^+$ cells after treatment SAG. Scale bars, 50 μm.

(F) Representative images and quantification of the projected cortical areas in E16.5 WT, *Eed* cKO, *Ptch1* cKO, and *Eed* cKO/*Ptch1* cKO (dcKO) mouse brains. Scale bar, 50 mm; n = 3 mice per group.

(G) Represent images and quantification of the number of $BrdU^+$ cells in cortices of E16.5 *Eed* cKO and WT mice that were subjected to SAG treatment and to BrdU pulse-chase labeling. Scale bars, 50 μm.

(H) Representative images and quantification of the number of $TUJ1^+$ cells in the cortices of E16.5 WT, *Eed* cKO, *Ptch1* cKO, and dcKO mice. Cortices were stained for Pax6 (green), Tuj1 (red) and DAPI (blue). Scale bars, 50 μm; n = 3 mice per group. Data are presented as means ± standard error of the mean; two-tailed unpaired t-test, n.s., non-significant, *p < 0.05, **p < 0.01, ***p < 0.001.

Writing - review and editing: C.M.L., X.G.L, Y.T.; Supervision: C.M.L., Y.T.

ACKNOWLEDGMENTS

The authors gratefully acknowledge Dr. Stuart H. Orkin at Harvard Medical School for providing $Eed^{fl/fl}$ mice. This work was supported by grants from the National Key Research and Development Program of China Project (2021YFA1101402/2018YFA0108001), the Strategic Priority Research Program of the Chinese Academy of Sciences (No. XDA16010302/XDA16021400), and the National Science Foundation of China (31900690).

CONFLICTS OF INTEREST

The authors declare no competing interests.

Received: January 7, 2022
Revised: July 6, 2022
Accepted: July 7, 2022
Published: August 4, 2022

REFERENCES

Agirman, G., Broix, L., and Nguyen, L. (2017). Cerebral cortex development: an outside-in perspective. FEBS Lett. *591*, 3978–3992.

Ai, S., Peng, Y., Li, C., Gu, F., Yu, X., Yue, Y., Ma, Q., Chen, J., Lin, Z., Zhou, P., et al. (2017). EED orchestration of heart maturation through interaction with HDACs is H3K27me3-independent. Elife *6*, e24570.

Al-Salem, A., Alshammari, M.J., Hassan, H., Alazami, A.M., and Alkuraya, F.S. (2013). Weaver syndrome and defective cortical development: a rare association. Am. J. Med. Genet. *161A*, 225–227.

Aprea, J., Prenninger, S., Dori, M., Ghosh, T., Monasor, L.S., Wessendorf, E., Zocher, S., Massalini, S., Alexopoulou, D., Lesche, M., et al. (2013). Transcriptome sequencing during mouse brain development identifies long non-coding RNAs functionally involved in neurogenic commitment. EMBO J. *32*, 3145–3160.

Belgacem, Y.H., Hamilton, A.M., Shim, S., Spencer, K.A., and Borodinsky, L.N. (2016). The many hats of sonic hedgehog signaling in nervous system development and disease. J. Dev. Biol. *4*, E35.

Boyer, L.A., Plath, K., Zeitlinger, J., Brambrink, T., Medeiros, L.A., Lee, T.I., Levine, S.S., Wernig, M., Tajonar, A., Ray, M.K., et al. (2006). Polycomb complexes repress developmental regulators in murine embryonic stem cells. Nature *441*, 349–353.

Bragina, O., Sergejeva, S., Serg, M., Zarkovsky, T., Maloverjan, A., Kogerman, P., and Zarkovsky, A. (2010). Smoothened agonist augments proliferation and survival of neural cells. Neurosci. Lett. *482*, 81–85.

Branzei, D., and Foiani, M. (2010). Maintaining genome stability at the replication fork. Nat. Rev. Mol. Cell Biol. *11*, 208–219.

Cayuso, J., Ulloa, F., Cox, B., Briscoe, J., and Martí, E. (2006). The Sonic hedgehog pathway independently controls the patterning, proliferation and survival of neuroepithelial cells by regulating Gli activity. Development (Cambridge, England) *133*, 517–528.

Chaudhry, P., Singh, M., Triche, T.J., Guzman, M., and Merchant, A.A. (2017). GLI3 repressor determines Hedgehog pathway activation and is required for response to SMO antagonist glasdegib in AML. Blood *129*, 3465–3475.

Cohen, A.S., and Gibson, W.T. (2016). EED-associated overgrowth in a second male patient. J. Hum. Genet. *61*, 831–834.

Cohen, A.S.A., Tuysuz, B., Shen, Y., Bhalla, S.K., Jones, S.J.M., and Gibson, W.T. (2015). A novel mutation in EED associated with overgrowth. J. Hum. Genet. *60*, 339–342.

Conway, E., Healy, E., and Bracken, A.P. (2015). PRC2 mediated H3K27 methylations in cellular identity and cancer. Curr. Opin. Cell Biol. *37*, 42–48.

Derwińska, K., Smyk, M., Cooper, M.L., Bader, P., Cheung, S.W., and Stankiewicz, P. (2009). PTCH1 duplication in a family with microcephaly and mild developmental delay. Eur. J. Hum. Genet. *17*, 267–271.

Gibson, W.T., Hood, R.L., Zhan, S.H., Bulman, D.E., Fejes, A.P., Moore, R., Mungall, A.J., Eydoux, P., Babul-Hirji, R., An, J., et al. (2012). Mutations in EZH2 cause Weaver syndrome. Am. J. Hum. Genet. *90*, 110–118.

Guillemot, F., Molnár, Z., Tarabykin, V., and Stoykova, A. (2006). Molecular mechanisms of cortical differentiation. Eur. J. Neurosci. *23*, 857–868.

Ji, F., Wang, W., Feng, C., Gao, F., and Jiao, J. (2021). Brain-specific Wt1 deletion leads to depressive-like behaviors in mice via the recruitment of Tet2 to modulate Epo expression. Mol. Psychiatry *26*, 4221–4233.

Julian, L.M., Vandenbosch, R., Pakenham, C.A., Andrusiak, M.G., Nguyen, A.P., McClellan, K.A., Svoboda, D.S., Lagace, D.C., Park, D.S., Leone, G., et al. (2013). Opposing regulation of Sox2 by cell-cycle effectors E2f3a and E2f3b in neural stem cells. Cell Stem Cell *12*, 440–452.

Komada, M., Iguchi, T., Takeda, T., Ishibashi, M., and Sato, M. (2013). Smoothened controls cyclin D2 expression and regulates the generation of intermediate progenitors in the developing cortex. Neurosci. Lett. *547*, 87–91.

Komada, M., Saitsu, H., Kinboshi, M., Miura, T., Shiota, K., and Ishibashi, M. (2008). Hedgehog signaling is involved in development of the neocortex. Development *135*, 2717–2727.

Lavado, A., Park, J.Y., Paré, J., Finkelstein, D., Pan, H., Xu, B., Fan, Y., Kumar, R.P., Neale, G., Kwak, Y.D., et al. (2018). The hippo pathway prevents YAP/TAZ-driven hypertranscription and controls neural progenitor number. Dev. Cell *47*, 576–591.e8.

Lee, Y., Katyal, S., Downing, S.M., Zhao, J., Russell, H.R., and McKinnon, P.J. (2012). Neurogenesis requires TopBP1 to prevent catastrophic replicative DNA damage in early progenitors. Nat. Neurosci. *15*, 819–826.

Li, L., Ruan, X., Wen, C., Chen, P., Liu, W., Zhu, L., Xiang, P., Zhang, X., Wei, Q., Hou, L., et al. (2019). The COMPASS family protein ASH2L mediates corticogenesis via transcriptional regulation of wnt signaling. Cell Rep. *28*, 698–711.e5.

Li, Y., and Jiao, J. (2017). Histone chaperone HIRA regulates neural progenitor cell proliferation and neurogenesis via beta-catenin. J. Cell Biol. *216*, 1975–1992.

Liu, P.P., Tang, G.B., Xu, Y.J., Zeng, Y.Q., Zhang, S.F., Du, H.Z., Teng, Z.Q., and Liu, C.M. (2017). MiR-203 interplays with polycomb repressive complexes to regulate the proliferation of neural stem/progenitor cells. Stem Cell Rep. *9*, 190–202.

Liu, P.P., Xu, Y.J., Dai, S.K., Du, H.Z., Wang, Y.Y., Li, X.G., Teng, Z.Q., and Liu, C.M. (2019a). Polycomb protein EED regulates neuronal differentiation through targeting SOX11 in hippocampal dentate gyrus. Stem Cell Rep. *13*, 115–131.

Liu, Z., Wang, X., Jiang, K., Ji, X., Zhang, Y.A., and Chen, Z. (2019b). TNFalpha-induced up-regulation of Ascl2 affects the differentiation and proliferation of neural stem cells. Aging Dis. *10*, 1207–1220.

Margueron, R., Justin, N., Ohno, K., Sharpe, M.L., Son, J., Drury, W.J., 3rd, Voigt, P., Martin, S.R., Taylor, W.R., De Marco, V., et al. (2009). Role of the polycomb protein EED in the propagation of repressive histone marks. Nature *461*, 762–767.

Margueron, R., and Reinberg, D. (2011). The Polycomb complex PRC2 and its mark in life. Nature *469*, 343–349.

Memi, F., Zecevic, N., and Radonjić, N. (2018). Multiple roles of Sonic Hedgehog in the developing human cortex are suggested by its widespread distribution. Brain Struct. Funct. *223*, 2361–2375.

Montgomery, N.D., Yee, D., Chen, A., Kalantry, S., Chamberlain, S.J., Otte, A.P., and Magnuson, T. (2005). The murine polycomb group protein Eed is required for global histone H3 lysine-27 methylation. Curr. Biol. *15*, 942–947.

MuhChyi, C., Juliandi, B., Matsuda, T., and Nakashima, K. (2013). Epigenetic regulation of neural stem cell fate during corticogenesis. Int. J. Dev. Neurosci. *31*, 424–433.

Paridaen, J.T.M.L., and Huttner, W.B. (2014). Neurogenesis during development of the vertebrate central nervous system. EMBO Rep. *15*, 351–364.

Pearson, C.A., Moore, D.M., Tucker, H.O., Dekker, J.D., Hu, H., Miquelajáuregui, A., and Novitch, B.G. (2020). Foxp1 regulates neural stem cell self-renewal and bias toward deep layer cortical fates. Cell Rep. *30*, 1964–1981.e3.

Pereira, J.D., Sansom, S.N., Smith, J., Dobenecker, M.W., Tarakhovsky, A., and Livesey, F.J. (2010). Ezh2, the histone methyltransferase of PRC2, regulates the balance between self-renewal and differentiation in the cerebral cortex. Proc. Natl. Acad. Sci. USA *107*, 15957–15962.

Schmitges, F.W., Prusty, A.B., Faty, M., Stützer, A., Lingaraju, G.M., Aiwazian, J., Sack, R., Hess, D., Li, L., Zhou, S., et al. (2011). Histone methylation by PRC2 is inhibited by active chromatin marks. Mol. Cell *42*, 330–341.

Shan, Y., Liang, Z., Xing, Q., Zhang, T., Wang, B., Tian, S., Huang, W., Zhang, Y., Yao, J., Zhu, Y., et al. (2017). PRC2 specifies ectoderm lineages and maintains pluripotency in primed but not naive ESCs. Nat. Commun. *8*, 672.

Smigiel, R., Biernacka, A., Biela, M., Murcia-Pienkowski, V., Szmida, E., Gasperowicz, P., Kosinska, J., Kostrzewa, G., Koppolu, A.A., Walczak, A., et al. (2018). Novel de novo mutation affecting two adjacent aminoacids in the EED gene in a patient with Weaver syndrome. J. Hum. Genet. *63*, 517–520.

Spellicy, C.J., Peng, Y., Olewiler, L., Cathey, S.S., Rogers, R.C., Bartholomew, D., Johnson, J., Alexov, E., Lee, J.A., Friez, M.J., and Jones, J.R. (2019). Three additional patients with EED-associated overgrowth: potential mutation hotspots identified? J. Hum. Genet. *64*, 561–572.

Stashinko, E.E., Clegg, N.J., Kammann, H.A., Sweet, V.T., Delgado, M.R., Hahn, J.S., and Levey, E.B. (2004). A retrospective survey of perinatal risk factors of 104 living children with holoprosencephaly. Am. J. Med. Genet. *128A*, 114–119.

Sun, B., Chang, E., Gerhartl, A., and Szele, F.G. (2018). Polycomb protein eed is required for neurogenesis and cortical injury activation in the subventricular zone. Cereb. Cortex *28*, 1369–1382.

Tang, T., Zhang, Y., Wang, Y., Cai, Z., Lu, Z., Li, L., Huang, R., Hagelkruys, A., Matthias, P., Zhang, H., et al. (2019). HDAC1 and HDAC2 regulate intermediate progenitor positioning to safeguard neocortical development. Neuron *101*, 1117–1133.e5.

Tatton-Brown, K., Murray, A., Hanks, S., Douglas, J., Armstrong, R., Banka, S., Bird, L.M., Clericuzio, C.L., Cormier-Daire, V., Cushing, T., et al. (2013). Weaver syndrome and EZH2 mutations: clarifying the clinical phenotype. Am. J. Med. Genet. *161A*, 2972–2980.

Telley, L., Agirman, G., Prados, J., Amberg, N., Fièvre, S., Oberst, P., Bartolini, G., Vitali, I., Cadilhac, C., Hippenmeyer, S., et al. (2019). Temporal patterning of apical progenitors and their daughter neurons in the developing neocortex. Science *364*, eaav2522.

Vizán, P., Beringer, M., Ballaré, C., and Di Croce, L. (2015). Role of PRC2-associated factors in stem cells and disease. FEBS J. *282*, 1723–1735.

Wang, L., Hou, S., and Han, Y.G. (2016a). Hedgehog signaling promotes basal progenitor expansion and the growth and folding of the neocortex. Nat. Neurosci. *19*, 888–896.

Wang, S., Sun, H., Ma, J., Zang, C., Wang, C., Wang, J., Tang, Q., Meyer, C.A., Zhang, Y., and Liu, X.S. (2013). Target analysis by integration of transcriptome and ChIP-seq data with BETA. Nat. Protoc. *8*, 2502–2515.

Wang, Y., Wu, Q., Yang, P., Wang, C., Liu, J., Ding, W., Liu, W., Bai, Y., Yang, Y., Wang, H., et al. (2016b). LSD1 co-repressor Rcor2 orchestrates neurogenesis in the developing mouse brain. Nat. Commun. *7*, 10481.

Wu, F., Zhang, Y., Sun, B., McMahon, A.P., and Wang, Y. (2017). Hedgehog signaling: from basic biology to cancer therapy. Cell Chem. Biol. *24*, 252–280.

Yoon, K.J., Ringeling, F.R., Vissers, C., Jacob, F., Pokrass, M., Jimenez-Cyrus, D., Su, Y., Kim, N.S., Zhu, Y., Zheng, L., et al. (2017). Temporal control of mammalian cortical neurogenesis by m(6)A methylation. Cell *171*, 877–889.e17.